Society For Biomaterials

Influence of a layer-by-layer-assembled multilayer of anti-CD34 antibody, vascular endothelial growth factor, and heparin on the endothelialization and anticoagulation of titanium surface

Shihui Liu,[1] Tao Liu,[1*] Junying Chen,[1] Manfred Maitz,[1,2] Cheng Chen,[1] Nan Huang[1]

[1]Key Laboratory of Advanced Technology for Materials of Chinese Education Ministry, School of Materials Science and Engineering, Southwest Jiaotong University, Chengdu, People's Republic of China
[2]Leibniz Institute of Polymer Research Dresden, Max Bergmann Center of Biomaterials, Hohe Str. 06, 01069 Dresden, Germany

Received 25 December 2011; revised 8 July 2012; accepted 23 July 2012
Published online 9 October 2012 in Wiley Online Library (wileyonlinelibrary.com). DOI: 10.1002/jbm.a.34392

Abstract: The endothelialization of the metal surface of vascular stents came into focus as a new method for improving the biocompatibility of intravascular stents. This article has its focus on building a biofunctional layer on the activated titanium surface with anti-CD34 antibody, vascular endothelial growth factor (VEGF), and heparin by a layer-by-layer (LBL) self-assembly technique, to promote the endothelialization of the surface. When compared with titanium surface, the number of adhered endothelial progenitor cells (EPCs) on LBLs increased 47.1% after 5 days culture, meanwhile the proliferation rate of EPCs on LBLs during 5 days culture also exhibit significantly improvement. The results of blood compatibility evaluation clearly show that the LBLs reduce the number of adhered and activated blood platelets (adhered: Ti 83% vs. LBL <20% and activated: Ti 57% vs. LBL 19%), and the activated partial thromboplastin time of the LBL surface prolonged about 20 s in compared with platelet-poor plasma. The assembled LBL thus improves the thromboresistance of the titanium surface. The presented biofunctional multilayer of anti-CD34, VEGF, and heparin on titanium can significantly improve the blood compatibility and the endothelialization of a medical device. The biofunctional layer supports generation of a new endothelium onto titanium surface by capturing EPCs and oriented differentiation. © 2012 Wiley Periodicals, Inc. J Biomed Mater Res Part A: 101A: 1144–1157, 2013.

Key Words: titanium, endothelialization, anticoagulation, anti-CD34 antibody, heparin, layer-by-layer assembly

How to cite this article: Liu S, Liu T, Chen J, Maitz M, Chen C, Huang N. 2013. Influence of a layer-by-layer-assembled multilayer of anti-CD34 antibody, vascular endothelial growth factor, and heparin on the endothelialization and anticoagulation of titanium surface. J Biomed Mater Res Part A 2013:101A:1144–1157.

INTRODUCTION

Cardiovascular diseases (CVDs) are widely known as a series of disorders that involve the heart or blood vessels and have been the leading killer globally. Currently, intravascular stenting has become an important therapy for stenosis in CVDs. In 2000, about 1.1 million patients undergo stent therapy in worldwide and this number increased to 2.1 million in 2005. Now, more than 4,000,000 stents were implanted into the human body annually. In china, the clinical demand of stents perhaps more surprising, with above 30% compound annual growth rate in clinical application amount of the stents, and in 2012, the clinical demand of stents will be increased over 800,000.

With the advantages of low density, high specific strength, excellent mechanical property, and adequate biocompatibility, titanium (Ti) and its alloys have been widely used for cardiovascular implants such as heart valves, artificial hearts, and vascular stents. However, the reported high thrombogenicity of Ti[1] constitutes a major drawback for successful application. Common approaches to solve the thrombosis problem, base on the construction of a bioactive and biological surface on the device, which supports endothelium growth, because endothelium is well known to present the best thromboresistant surface.

Soon after the first description of endothelial progenitor cells (EPCs) circulating in the blood,[2] many studies have shown that that EPCs are mobilized from bone marrow and recruited into injured tissues and contribute there to revascularization either by direct incorporation into vessel walls or by secreting a variety of angiogenic growth factors.[3] Thus, construct a biofunctional multilayer on biomaterial's surface to capture EPCs would contribute to generate a new endothelial layer. Early EPCs in the bone marrow or immediately after their migration into the systemic circulation

*This author contributed equally to this work.
Correspondence to: J. Chen; e-mail: chenjy@263.net
Contract grant sponsor: Key Basic Research Project; contract grant number: 2011CB606204
Contract grant sponsor: Natural Science Foundation of China; contract grant number: 31170916
Contract grant sponsor: Fundamental Research Funds for the Central University; contract grant number: SWJTU11ZT11

are positive for the surface markers CD34, CD133 (AC133) and vascular endothelial growth factor receptor 2 (VEGFR-2) receptor.[4] Subsequently, circulating EPCs obviously lose CD133 but remain positive for CD34, VEGFR-2, CD31, VE-cadherin, and von Willebrand factor (vWF).[4] Therefore, several studies have focused on immobilizing anti-CD34 antibodies on the stent surface, which preferentially captures circulating EPCs by recognizing their specific surface antigens. Kutryk and Kuliszewski[5] first coated rat monoclonal CD34 antibody on the 316LSS stent surface to precapture EPCs before implantation, and animal test results showed that confluent endothelial cell (EC) monolayer was formed after 48 h. Subsequently, first clinical trials in humans with anti-CD34 antibody-coated stents demonstrated that the EPC capture coronary stent is safe and feasible for the treatment of *de novo* coronary artery disease.[6] Hemodialysis grafts of expanded polytetrafluoroethylene had been immobilized with anti-CD34 antibody for *in vitro* colonization with ECs in pigs. Although significantly improved endothelialization was observed after 72 h, the treatment was associated with enhanced intimal hyperplasia after 4 weeks.[7]

Although EPCs play important part in the process of endothelialization, the quantity of the effective EPCs in circulating blood is very low at only 0.4 $\pm$ 0.2% of the total $CD34^+$ population.[4] It needs mobilization of EPCs from bone marrow to peripheral blood, which can be achieved by VEGF,[8] a subfamily of growth factors associated with EC differentiation and proliferation.[9] Asahara et al.[10] indicated that VEGF could induce the mobilization of EPCs from bone marrow into circulation and subsequent promote EPCs proliferation and differentiation by intraperitoneal injection of VEGF into mice. Crombez's[11] group immobilized the VEGF onto PTFE surfaces to favor the interaction with ECs. Pike et al.[12] also proved that VEGF could promote neovascularization and suggested that the addition of heparin in scaffolds may control the release of VEGF, retain their bioactivity and against degradation by ECM proteinases.

After stents are implanted into human's body, the problem of coagulation caused by the interaction between the implant and blood is always the main issue. Heparin is commonly used clinically as anticoagulant. It has an incontrovertible effect on suppressing subacute in-stent thrombus.[4] Heparin-coated stents frequently have been shown to exhibit satisfactory thromboresistance.[13–15]

Improved endothelialization and reduced thrombosis of cardiovascular devices by surface biomimetic microenvironment construction has become the focus. Recently, some technologies for the immobilization of bioactive molecules on titanium surfaces by layer-by-layer (LBL) self-assembly methods have been developed,[16–18] which may provide a new way in cardiovascular material surface multifunctional modification. Based on a charged surface, a monolayer of oppositely charged proteins adsorbs and further over-compensates the charge, leading to a charge reversal. Alternate charged layers of different proteins are subsequently deposited[16] for obtaining the LBL biofunctional layer. In this way, very versatile structures can be prepared using a multilayered architecture. It is our hypothesis in this article that immobilization of biomolecules with induce cell mobilization and regeneration functions (VEGF), specific recognition and capture characteristics (anti-CD34 antibody), as well as antithrombosis properties (heparin) to titanium surface LBL via intermolecular interactions might present better blood compatibility and endothelialization ability. The effect of LBL on EPCs adhesion and proliferation was investigated by *in vitro* cell culture assay, the blood compatibility of LBL-modified surface was characterized by platelet adhesion and activation, as well as activated partial thromboplastin time (APTT) test.

MATERIALS AND METHODS

Materials and reagents

The used materials are commercial pure Titanium (99.9%) purchased from Baoji Norferrous Metal (Shanxi Province, China). Phosphate buffer saline (PBS, 0.067 *M*, and pH 7.4) was used in all biofunctional protein solution preparation for LBL multilayer construction, as well as in sample rinsing. Goat anti-CD34 antibody and VEGF was from Santa CRUZ. Avidin (activity $\geq$ 10 U/mg and protein (%) $\geq$ 95%) was from Beijing Solarbio Science and Technology (Beijing, China). Biotinylated protein A, fluorescein isothiocyanate (FITC)-conjugated rabbit anti goat IgG, tetramethylrhodamine isothiocyanate (TRITC)-conjugated rabbit anti human VEGF antibodies, and rabbit serum were from Wuhan Boster Biological Technology (Wuhan, China). Biotinylated Heparin was prepared in the author's laboratory with the method referring to Weng.[19]

Fabrication of anti-CD34 antibody–VEGF–heparin LBL multilayer

Titanium discs with the size of 10 mm in diameter and 1 mm in thickness were treated by first sandpaper grinding and mechanical polishing to a mirror-like finish, and then were ultrasonically cleaned in a detergent solution, acetone, ethanol, and deionized water for 10 min each to remove oily dirt, and finally dried at 60°C. The cleaned samples were immersed in 4 *M* NaOH solution at 70°C for 20 h and followed by deionized water at 70°C for 24 h. The samples were then extensively rinsed with deionized water, and dried at 60°C, which resulted in a stable negatively charged substrate surface with Ti–OH. Then, the NaOH etched samples (Ti–OH) were immersed in a 0.1 mg/mL Avidin solution (PBS, pH 7.4) at 4°C for 12 h, subsequently rinsed three times in PBS for 5 min, and dried in air at room temperature. The avidin adsorbed substrates (Ti–OH–Avi) were then dipped into a 0.1-mg/mL biotinylated protein A and 1 mg/mL biotinylated heparin mixed solution (PBS, pH 7.4) at 4°C for 12 h, following the same rinsing and drying procedure as before. The protein A and the heparin allow the subsequent immobilization of the anti-CD34 antibody and VEGF, which is based on the specific affinity of protein A and IgG antibodies,[20] heparin, and VEGF.[21] The biotinylated samples (Ti–OH–Avi–(Bio-A + Bio-H)) were finally immersed in a 2 μg/mL anti-CD34 antibody and 0.2 μg/mL VEGF mixed solution (PBS, pH 7.4) at 4°C for 12 h, contiguously the same rinsing and dry procedure. The samples

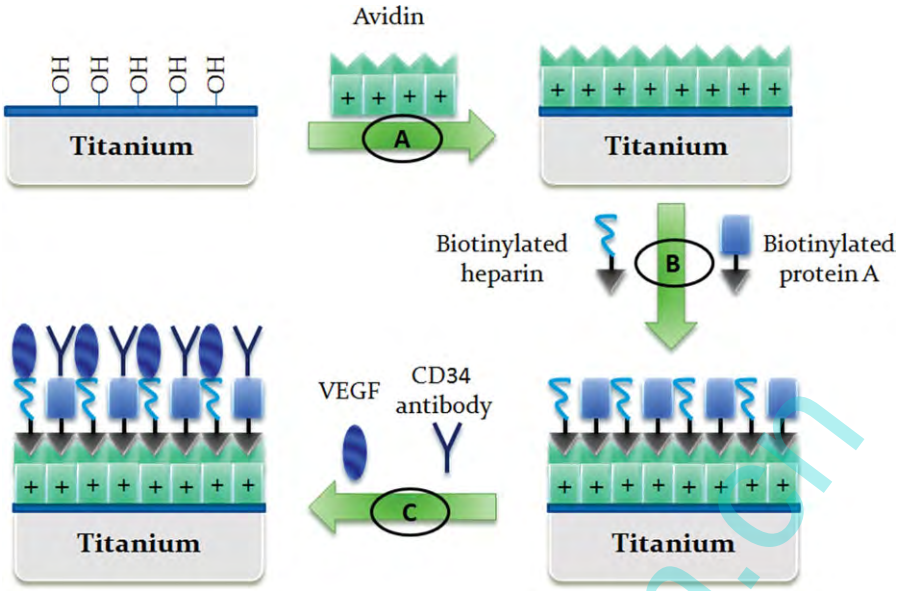

FIGURE 1. The model of Layer-by-layer self-assembling multilayer. A: Ti treated with alkali to acquire a negative charged surface and positively charged avidin bond to the surface by electrostatic adsorption, (B) biotinylated heparin and protein A are immobilized by biotin-avidin system, (C) VEGF and CD34 antibody are oriented assembled on the surface via intermolecular interactions. [Color figure can be viewed in the online issue, which is available at wileyonlinelibrary.com.]

were denoted as Ti–OH–Avi–(Bio-A + Bio-H)–(CD34 + VEGF) or LBL. The LBL self-assembling multilayer model is shown in Figure 1. All the samples were prepared to three parallel samples for subsequent experiments.

Characterization of the LBL self-assembly multilayer

FTIR. The chemical composition of LBL self-assembly multilayer was investigated by Fourier transform infrared spectroscopy (FTIR) (NICOLET 5700 infrared spectroscopy) with the mode of diffuse reflectance. Scanning was conducted in the range from 400 to 4000 cm^{-1}.

Immunofluorescence. Immunofluorescence was used for further demonstrating the assembled biomolecules. To justify the successful fabrication of biotinylated protein A and biotinylated heparin, the Ti–OH–Avi, Ti–OH–Avi–(Bio-A), Ti–OH–Avi–(Bio-H) and the Ti–OH–Avi–(Bio-A + Bio-H) samples were stained by FITC-labeled streptavidin with fluorescence microscopic (DMRX, Leica, German) observation. To identify anti-CD34 antibody and VEGF, respectively, the LBL samples were stained by double fluorescence as follows. The LBL samples were firstly immersed into rabbit serum (1:10 diluted in PBS) for 30 min at 37°C to block nonspecific adsorptions, lastly the sample rinsed with PBS. Subsequently the FITC-rabbit anti-sheep IgG and TRITC-rabbit anti human VEGF antibodies were introduced onto the samples for 1 h at 37°C and rinsed with PBS.

AFM. The changes of the surface morphology and roughness of Ti, Ti–OH, and the LBL samples were investigated by atom force microscopy (AFM). Arithmetic average roughness (Ra), root mean square (Rms), and the Ten Point Height (Sz) were common used parameters to express the surface roughness. Ra and Rms were the arithmetical mean of the absolute values, and the Rms average of roughness profile ordinates, respectively. Sz was defined as the average height of the five highest local maximums plus the average height of the five lowest local minimums. The Ra, Rms, and Sz values of different samples were calculated by using the CSPM imager software.

Water contact angle. To verify the alterations of the surface hydrophilicity, the samples were characterized by static water contact angle measurements using Krüss GmbH DSA 100 Mk 2 goniometer.

QCM-D measurement of the LBL self-assembly multilayer

A Q-Sense E4 instrument was used to monitor the LBL multilayer buildup. *In situ* quartz crystal microbalance with dissipation (QCM-D) analysis mode was used as reported.[22] The quartz crystal is excited at its fundamental frequency (~5 MHz, $v = 1$), as well as at the 3rd, 5th, 7th, and 9th overtones ($v = 3$, 5, 7, and 9, corresponding to 15, 25, 35, and 45 MHz, respectively). Changes in the resonance frequencies (ΔF) and in the relaxation (ΔD) of the vibration were recorded at the five frequencies once the excitation is stopped.[23]

In detail, the gold-plated quartz crystal surfaces were cleaned in solution (H_2O_2/H_2SO_4—3:7, v/v) for 5 min, and then washed thoroughly with absolute ethanol and distilled ultrapure water. The gold-plated substrate immediately immersed in 50 m*M* 3-mercaptopropionic acid (MPA) aqueous solution. The gold-plated slide was taken from the solution after 24 h, thoroughly rinsed in absolute ethanol and ultrapure water and allowed to dry.[24] After the gold-plated

plates treated by MPA were mounted in the QCM chamber, the PBS was injected for equilibration. Thereafter, a solution of 0.2 mol/L N-(3-dimethy laminopropyl)-N′-ethylcarbodiimide and 0.05 mol/L N-hydroxysuccinimide was injected at 50 μL/min for 10 min to activate the carboxyl groups into reactive N-hydroxysuccinimate esters.[24] Then, the avidin solution was continuously injected at 50 μL/min until the QCM indicated equilibrium, followed by the buffer pump at the same speed. Then, the biotinylated protein A and biotinylated heparin mixed solution were injected at the same speed until equilibrium and followed by the buffer pump at the same speed. Finally, the anti-CD34 antibody and VEGF mixed solution were injected into the chamber at the same speed until equilibrium again and followed by the PBS at the same speed. Frequency shift versus time (Δf–t) curves were recorded to monitor the stability of the adsorbed multilayer. All measurements were performed at 37°C.

In vitro EPCs culture

Cells were isolated and cultivated from bone marrow of Sprague-Dawley (SD) rat (from Sichuan University, Chengdu, China)[20] and cultured according to Ref. [25]. First, the bone marrow of SD rat was extracted and blown into suspension cells with α-Modified Eagle's Medium (α-MEM) containing 20% fetal bovine serum (FBS), which were cultivated in single-use culture bottle and incubated at 37°C under 5% CO_2. The medium was changed every 2 days. When over grown, cells were trypsinized to passage and cultured in α-MEM supplemented with 20% FBS and 20 ng/mL VEGF. Cells at passage 2 are designated as EPCs according to their morphology and positive expression of the markers CD34 and VEGF receptor-2 (VEGFR-2) by immunofluorescence assay with the same procedure as described in "Immunofluorescence" section.

EPCs were then seeded on the titanium dishes surface modified by the LBL self-assembled multilayer in a 24-well plate at density of 1×10^5/mL, and incubated at 37°C under 5% CO_2. For evaluating the cell affinity of the anti-CD34 antibody–VEGF–heparin LBL coating, the Ti and non-assembled Ti–OH samples were chosen as controls. All samples were sterilized under ultraviolet radiation (27 W, wavelength 254 nm) for 30 min before cell seeded. After cultured for 1 day, 3 days, and 5 days, the adherent cells on samples were fixed with 2.5% glutaraldehyde solution for 6 h at 4°C and rinsed with PBS, and then the adherent cells on samples were observed via the expression of a kind of cytoskeleton of actin with immunofluorescent staining.[26]

The EPCs metabolic activity on the samples was investigated by Alamar Blue test according to Ref. 25. After the EPCs were seeded onto the samples in 24-well plate for 1 day, 3 days, and 5 days in a cell incubator (at 37°C and 5% CO_2), the phenol red-free medium (1 mL) containing 10% Alamar Blue solution was added into the wells, and incubated for 4 h. Then, 200 μL Alamar Blue solution of the cells was transferred into a 96-well plate, and the absorbance of the solution corresponded to the different samples was measured at wavelength of 570 nm (A_{570}) and 600 nm (A_{600}) using a microplate reader. The reduced Alamar Blue (AR) was calculated according to the following formula.[25]

$$AR_{570} = [A_{570} - A_{600} \times 0.69] \quad (1)$$

In vitro hemocompatibility evaluation

In vitro platelet adhesion. For platelet adhesion studies, the platelet-rich plasma (PRP) was prepared by centrifuging (1500 rpm, 15 min) fresh human whole blood (Supplied by Chengdu City Blood Centre, Chengdu, China) containing 3.8 wt % citrate ($Na_3C_6H_5O_7 \cdot H_2O$) solution (blood:citrate solution = 9:1, v/v) obtained from healthy volunteers after informed consent. The 400 μL PRP was carefully added onto the LBL sample surfaces placed in a covered 24-well plate, immediately located in an incubator shaking at 37°C. The Ti and Ti–OH samples were used as comparison. After incubation for 0.5 h and 2 h, the samples were removed and gently rinsed three times with PBS to remove platelets adsorbed nonspecifically on the surface, and then dipped into 2.5% glutaraldehyde solution for 6 h at room temperature and followed with PBS rinsing. Samples were then dehydrated with 50%, 75%, 90%, and 100% mixtures of ethanol in water, and dealcoholized with 50%, 75%, 90%, and 100% mixtures of isoamyl acetate in ethanol. The samples were subsequently dried by critical point drying with CO_2. All the samples were coated with a gold layer and observed with SEM.

The quantity of platelet adhesion on the sample surface was determined by lactate dehydrogenase (LDH) assay.[27] In details, 40 μL PRP obtained by the same method above was carefully added onto the sample surfaces placed in a 24-well plate and incubated at 37°C for 45 min. After the samples were rinsed three times with PBS, the adherent platelets on sample surfaces were covered by 40 μL Triton X-100 (diluted to 1%) at 37°C for 5 min, then, 25 μL lysate of that was taken from the surfaces and mixed with 200 μL tris(hydroxymethyl)aminomethane base buffer mixture containing 0.28 mg/mL nicotinamide adenine dinucleotide reduced (NADH) and 0.187 mg/mL pyruvate in a 96-well plate. Thereafter, the absorbance of LDH from every well was determined using microplate reader at 340 nm. Finally, the LDH activation of adherent platelets on sample surfaces was evaluated by a calibration curve made by using the LDH activity of lysed platelet suspensions of known concentration.

In vitro platelet activation. The platelet activation induced by sample surfaces was measured using immunofluorescence of p-selectin also called GMP-140.[28] First, sample surfaces were covered by 40 μL PRP and incubated at 37°C for 2 h, and then were fixed with 2.5% glutaraldehyde in PBS for 2 h and subsequently washed with PBS for 5 min. After that, 1 mL 5% sheep serum was added onto the surfaces and incubated at 37°C for 30 min to block nonspecific adsorption. Then, 20 μL monoclonal mouse anti-human antibody against platelet p-selectin (1:100) (first antibody) was added to surfaces at 37°C for 1 h and washed with PBS for 5 min 3 times. Later, 20 μL Cy3 labeled monoclonal sheep

anti-mouse IgG antibody (second antibody) (1:100) was added to the surfaces at 37°C for 1 h and washed with PBS for 5 min 3 times. Finally, the samples were observed by fluorescence microscopy.

In addition, platelet activation on sample surfaces was also measured by immunochemistry assay for p-selectin (GMP-140).[27] The procedure of incubated PRP and first antibody on samples was the same as immunofluorescence. After the first antibody added, 20 μL peroxidase-conjugated monoclonal sheep anti-mouse IgG antibody (second antibody) (1:100) was added to the surface of the samples incubated for 1 h at 37°C and then washed with PBS for 5 min 3 times. A 60 μL of 3,30,5,50-tetramethylbenzidine chromogenic solution was added to the surfaces and reacted for 10 min, which was stopped by adding 50 μL of 2 *M* H_2SO_4. Finally, 100 μL of the reacting solution was taken into a 96-well plate. The absorbance was measured at 452 nm using microplate reader. The GMP-140 activation of adherent platelets on sample surfaces was evaluated by a calibration curve made by using the second antibody of known concentration. Ti and Ti–OH samples were used as comparison.

Activated partial thromboplastin time. The human platelet-poor plasma (PPP) was prepared by centrifuging the PRP at 3000 rpm for 15 min. A 400 μL PPP was carefully added onto the surface of LBL samples placed in a 24-well plate, and were incubated for 30 min at 37°C. Blank PPP, Ti, and Ti–OH samples served as control. Then, 100 μL PPP were taken out the well into test tubes adding 100 μL actin-activated cephthaloplastin reagents, and incubated for 3 min at 37°C. Then, 100 μL 0.025 *M* $CaCl_2$ solution was added into the testing tubes. The clotting time (APTT) was automatically measured by a coagulometer system (Clot 1A, Innova Co., Italy).

Statistical analysis

At least three independent experiments were performed for the assay described above. The results were expressed as a mean ± standard deviation (std) for each sample. Each experiment was repeated independently four times. One-way ANOVA in origin 6.0 (Microcal) was used to compare the data obtained from the different samples under identical treatments. A value of $*p < 0.05$ was considered significant.

RESULTS

Characterizations of the LBL self-assembly multilayer

FTIR. Figure 2 shows the FTIR spectra of the LBL self-assembly multilayer. The scanning range was from 4000 cm^{-1} to 400 cm^{-1}. Comparing to the spectra of the untreated Titanium [Fig. 2(A)], the NaOH etched titanium obviously shows a broad peak at about 3327 cm^{-1} [Fig. 2(B)], which is the characteristic region of hydroxyl groups (—OH) vibrations.[19] This proves that the hydroxyl groups are presented on titanium surface etched by NaOH solution. Although the surface is assembled with the protein avidin [Fig. 2(C)], two new peaks are observed at about 1649 cm^{-1} and about 1543 cm^{-1}, which corresponding to the C=O of amide I bond and the C—N, N—H of amide II bond.[20] After the biotinylated protein A and biotinylated heparin are added to the surface [Fig. 2(D)], there are the same two peaks at about 1649 cm^{-1} and about 1543 cm^{-1} due to the identical functional group of protein. However, a new peak at 1090 cm^{-1} is appeared, which is ascribed to the —C—O—C— bond of heparin.[28] After the anti-CD34 antibody and the VEGF are assembled to the surface, no new peaks are found except the enhance of the two peaks at about 1649 cm^{-1} and about 1543 cm^{-1}, as shown in Figure 2(E). So, for demonstrating the effective immobilization of the anti-CD34 antibody and the VEGF, the immunofluorescence staining of the assembled biomolecule is further adopted.

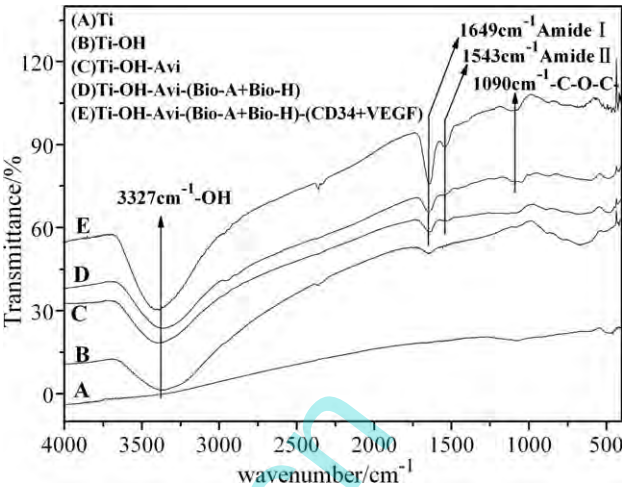

FIGURE 2. The FTIR spectra of the different samples with (A) Ti, (B) Ti–OH, (C) Ti–OH–Avi, (D) Ti–OH–Avi–(Bio-A + Bio-H), and (E) Ti–OH–Avi–(Bio-A + Bio-H)–(CD34 + VEGF).

Immunofluorescence staining. Based on the specific combination of antigen–antibody, the immunofluorescence staining is widely used to detect antibody. Immunofluoresence in the assay was amplified using an indirect system with biotin conjugated antibodies, and it is also found that the biotin/avidin system is a very good example of biomolecular recognition with a very high affinity constant ($K_a \sim 10^{15}$ M^{-1}) and specificity.[29] The biotin is easily labeled with protein molecules, and the biotin/avidin system is usually used as a new fluorescence method for characterizing protein. The immunofluorescence staining results of different samples are showed in Figures 3 and 4. Comparing to the nonbiotinylated sample of Ti–OH–Avi [Fig. 3(A)], the green fluorescence could be clearly observed on samples Ti–OH–Avi–(Bio-A) [Fig. 3(B)], Ti–OH–Avi–(Bio-H) [Fig. 3(C)], and Ti–OH–Avi–(Bio-A + Bio-H) [Fig. 3(D)]. This confirms that the biotinylated protein A and biotinylated heparin were successfully assembled to the surface either as single molecule or mixed molecule. After the anti-CD34 antibody and the VEGF were assembled to the surface of LBL sample, the green and the red fluorescence in Figure 4(A,B) also differently demonstrate that the assembling of anti-CD34 antibody and VEGF was successful, respectively. The FTIR and fluorescence staining results show that the biofunctional layers are assembled successfully.

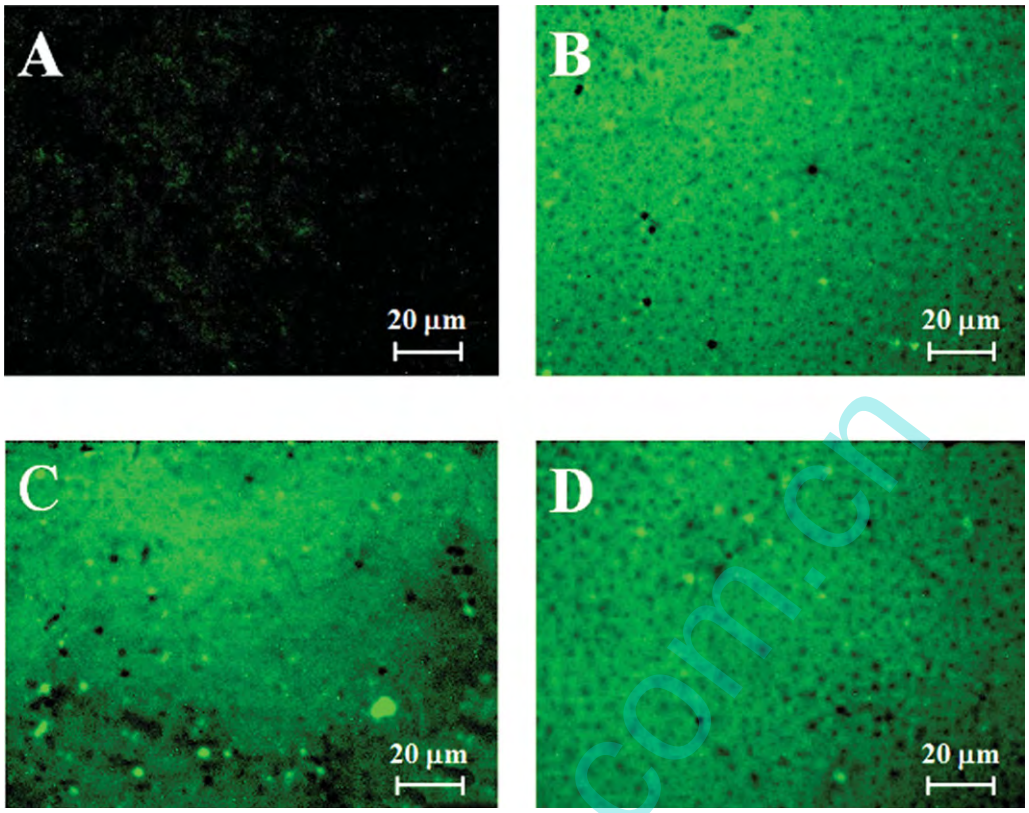

FIGURE 3. Immunofluorescence images of samples (A) Ti–OH–Avi, (B) Ti–OH–Avi–(Bio-A), (C) Ti–OH–Avi–(Bio-H), and (D) Ti–OH–Avi–(Bio-A + Bio-H). [Color figure can be viewed in the online issue, which is available at wileyonlinelibrary.com.]

Surface investigation using AFM. As far as biomaterial interactions with proteins are concerned, surface features in the nanometer scale are important.[30] AFM images show the topography of the sample surface in Figure 5. The titanium surface presents a smooth morphology [Fig. 5(A1)], after NaOH etched, the surface becomes rougher and composed of many taper-pointed granules forming morphology of valleys and peaks due to the alkali washing [Fig. 5(B1)]. The biomolecule assembled the sample appear to be smoother than the Ti–OH sample [Fig. 5(C1)]. The three-dimensional AFM images can also display the changes of the topography of the samples clearly [Fig. 5(A2–C2)]. The arithmetic average surface roughness of Ti–OH and LBL were 65 nm and 49 nm, respectively (Table I), about 5–10-fold of the size of adhesive proteins (2–10 nm). The increase in surface roughness contributes to provide more area for proteins adhesion.[30]

Water contact angle measurement. Surface hydrophilicity of a biomaterial is a key factor to influence the biocompatibility.[31] The result of the water contact angle of the LBL self-assembly multilayer is given in Figure 6. After NaOH solution etching, the water contact angle of titanium surface is significantly decreased due to the presence of hydroxyl groups. The hydroxyl groups are known to enhance the reactivity of titanium with the protein.[32] Although the molecules of avidin, biotinylated protein A and biotinylated heparin were immobilized onto the surface, the contact angles changed from 12.1° to 18.0°; but after the anti-CD34 antibody and VEGF assembled, the contact angle shows significant increase. This is because the exposed hydroxyl groups were covered by the biomolecule film and the wettability was determined by hydrophilic side chains of proteins and the heparin.[27]

QCM-D measurement

The process of LBL self-assembled multilayer was monitored by QCM-D. Changes of frequency versus time are recorded in Figure 7. The data are then transformed into the mass changes of adhesion protein with time by the soft QCP401 according to the Sauerbrey equation.

$$\Delta m = -\Delta f \times \frac{C}{n} \tag{2}$$

where Δf is the changes of frequency, C (=17.4 ng cm^2 Hz^{-1} at $f_{n=1}$ = 5 MHz) is the mass sensitivity constant and n (=1, 3, ...) is the overtone number. Figure 7 shows the mass changes of adhesion biomolecule with time. With each assembling of the biomolecule, there is a sharp increase (denoted with arrows) in mass, which indicates the adsorption of the biomolecule onto the gold-plated quartz crystal surface. The ladder form of the curve of mass changes proves the LBL structure of the self-assembling multilayer. However, with the each washing of PBS in self-

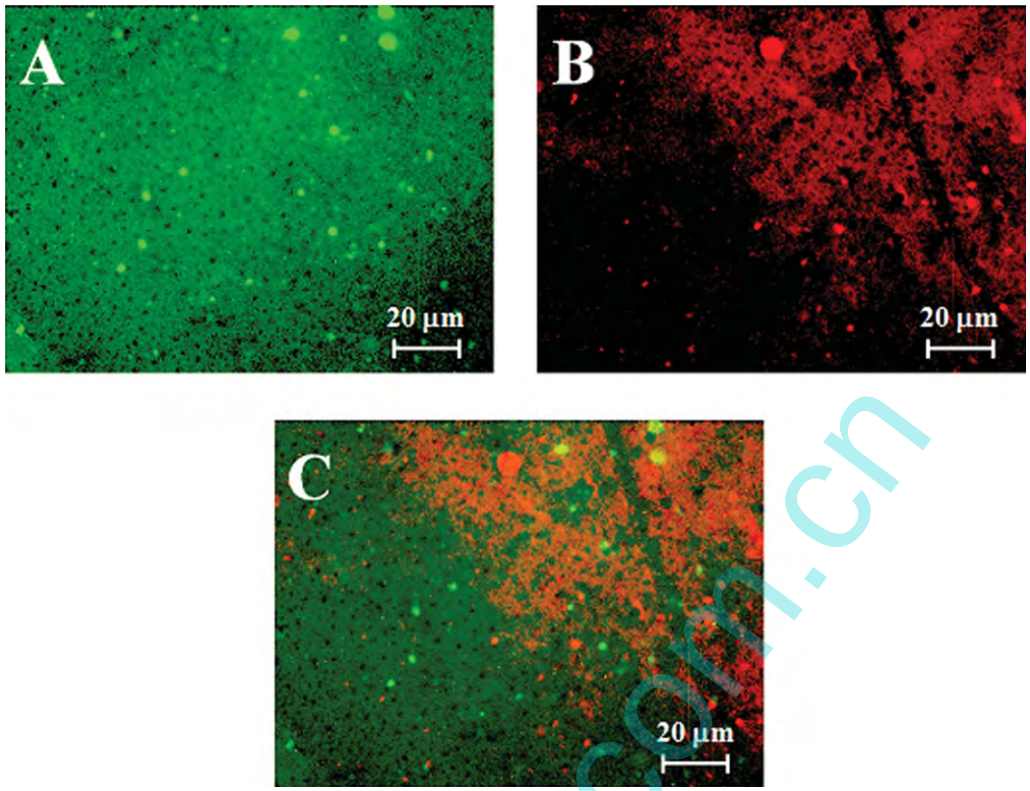

FIGURE 4. Immunofluorescence images of LBL (A) anti-CD34 antibody, (B) VEGF, and (C) merged image. [Color figure can be viewed in the online issue, which is available at wileyonlinelibrary.com.]

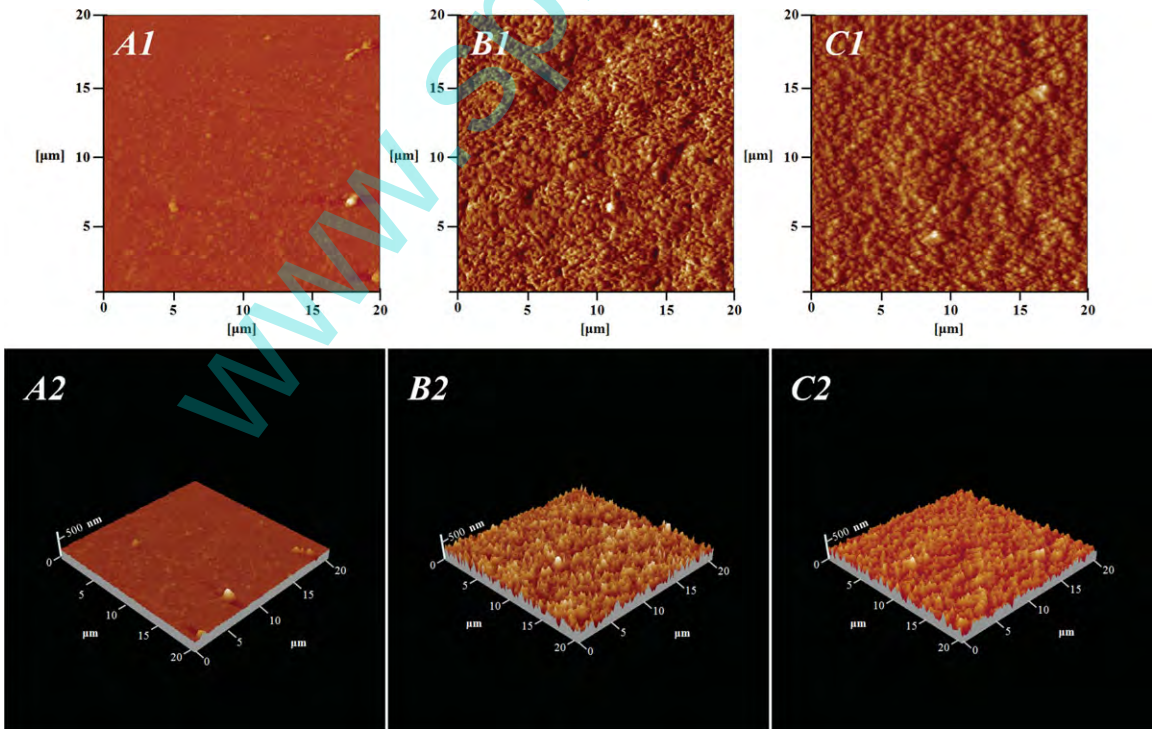

FIGURE 5. AFM images of the different samples with (A1 and A2) Ti, (B1 and B2) Ti–OH, and (C1 and C2) LBL. [Color figure can be viewed in the online issue, which is available at wileyonlinelibrary.com.]

TABLE I. The Roughness of the Samples Surface Measured by AFM

	Ti	Ti–OH	LBL
Ra (nm)	3 ± 0.2	65 ± 7	49 ± 8
Rms (nm)	5 ± 0.4	80 ± 2	62 ± 1
Sz (nm)	138 ± 17	562 ± 39	471 ± 23

assembling process, there is a desorption process of biomolecule (denoted by arrows). The masses of each adhesion biomolecule of avidin, bio-A and Bio-H, anti-CD34, and VEGF on quartz crystal gold surface are calculated and given in Table II.

EPCs culture result

Actin is the main component of the cytoskeletal system that allows movement of cells and cellular processes. It works in conjunction or in tandem with other components of the system.[25] Figure 8 shows the FITC-immunofluorescence images of the actin cytoskeleton of cultivated EPCs on the sample surfaces of Ti, Ti–OH, and LBL at different points of time. It is obvious that, from 1 day, 3 days, to 5 days seeding, the number of adhered EPCs on Ti and Ti–OH sample surface is significantly lower than that on LBL surface. The morphology of EPCs on LBL-assembled surface is fusiform after 1 day culture, and then the EPCs rapidly grow and spread to forming a confluent monolayer layer after 5 days. On the Ti and Ti–OH sample surfaces, the adhered EPCs were less, some of those were round and did not spread. Apparently, the assembled biofunctional layers improve the adhesion and proliferation of EPCs.

Alamar Blue results [Fig. 9(A)] show that the amount of reduced dye (AR) increased 47.1% after 5 days cell culture on the multilayer in compared with that Ti samples. Moreover, the normalized results [Fig. 9(B)] also show that the AR was significantly increased on the LBL surface in day 5, indicating higher metabolic activity of EPC on LBL-assembled sample surface than on the controls. The proliferation of the EPCs on the reference Ti and Ti–OH surface was relatively low, which may due to the low attachment in the early period. This result confirms the behavior of EPCs observed by immunofluorescence.

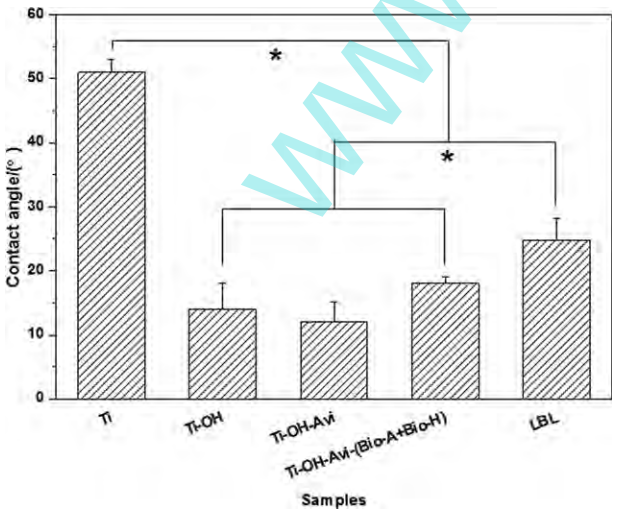

FIGURE 6. Contact angle of LBL self-assembly multilayer with water ($N = 4$, mean ± std, and $*p < 0.05$).

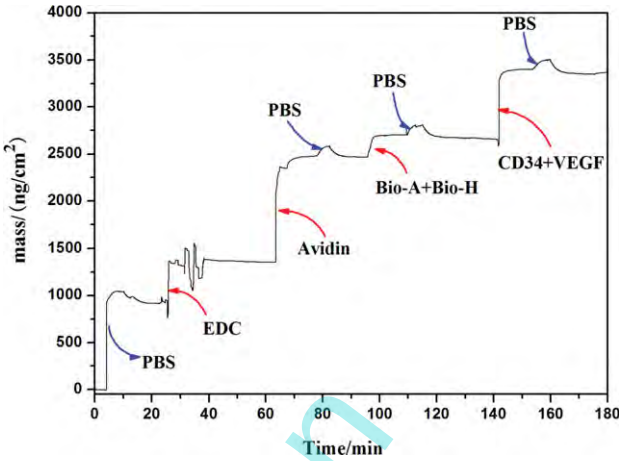

FIGURE 7. Mass versus time curve of LBL multilayer constructed onto a silicon-gold-coated quartz crystal. [Color figure can be viewed in the online issue, which is available at wileyonlinelibrary.com.]

Platelet adhesion

Platelets under normal circumstances will neither adhere to healthy arterial walls nor be activated by the vascular endothelium. However, platelets will adhere to the endothelium and be activated at the site of injury after stent implantation and trigger the recruitment of more platelets forming thrombosis.[25] Thus, platelet adhesion experiment is an important method to evaluate the hemocompatibility of the vascular implant biomaterials. The SEM images (Fig. 10) show the adherent platelets on the LBL-assembled layers incubated for 0.5 h and 2 h, Ti and Ti–OH samples are also shown for comparison. After incubation for 0.5 h, the number of adherent platelets on the LBL-assembled surface was lower than that on the control samples. In addition, the platelet morphology indicates a more resting state; especially on titanium the platelets adhere wide spread. However, although heparin is assembled to Ti surface, the heparin could restrain the adhesion and activation of platelets. The results are consistent with observations reported by others.[13,33] After incubation for 2 h, there were more aggregates and pseudopodia of platelets on Ti and Ti–OH surface, but the platelets on LBL surface remained mainly constant. In addition, quantification of the adherent platelets in the LDH assay confirm the anti-platelet effect of the LBL-assembled surface compared with the titanium and Ti–OH

TABLE II. Mass of Each Biomolecule Assembled on Quartz Crystal Gold Surface

	Biomolecule		
	Avidin	Bio-A + Bio-H	Anti-CD34 + VEGF
Mass (ng/cm²)	1112 ± 28	205 ± 19	693 ± 15

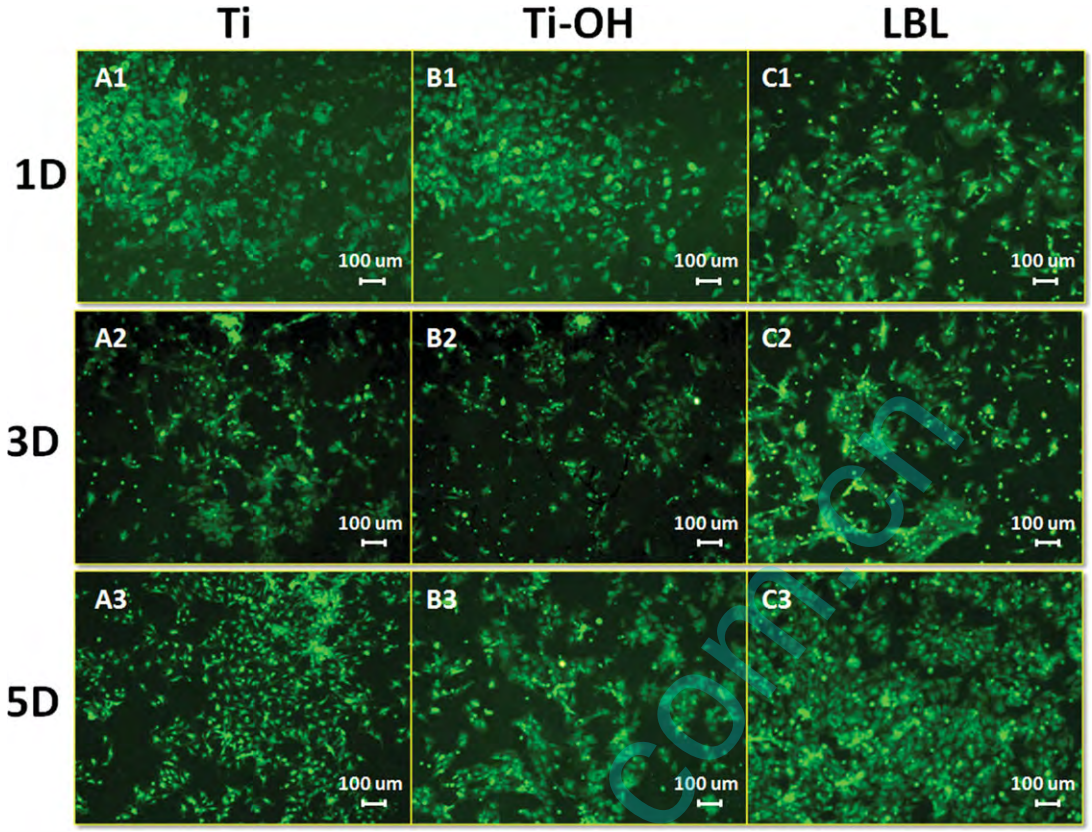

FIGURE 8. Actin immunofluorescence images of EPCs after cultured on different samples for 1 day, 3 days, and 5 days, respectively. [Color figure can be viewed in the online issue, which is available at wileyonlinelibrary.com.]

controls (Fig. 11). After the NaOH treated the titanium, the ratio of adherent platelets decreased from 83% to 57%, and again dropped to less than 20% with the biomolecules assembled.

Platelet activation

Figure 12 shows the activated platelets stained by p-selectin on different sample surface. It could be seen that there are a significantly larger amounts of activated platelets on control Ti and Ti–OH samples, whereas the LBL sample surface show less activated platelets. The ratio of activated platelets measured by ELISA onto different samples (as shown in Fig. 13) was similar to the immunofluorescence result. The ratio (57%) of activated platelets was highest on the Ti surface, and the ratio of activated platelets decreased to 47% on the NaOH treated titanium surface. For the modified sample

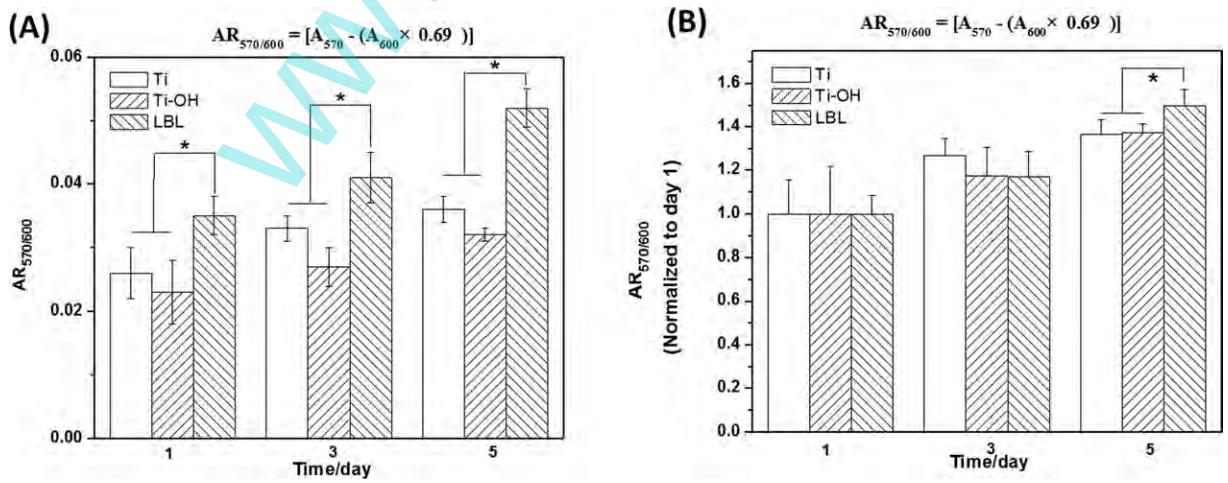

FIGURE 9. (A) Alamar Blue results of EPCs cultured on Ti, Ti–OH, and LBL samples for 1 day, 3 days, and 5 days, respectively and (B) Alamar Blue results on days 3 and 5 normalized to those on day 1. ($N = 4$, mean $\pm$ std, and $^*p < 0.05$).

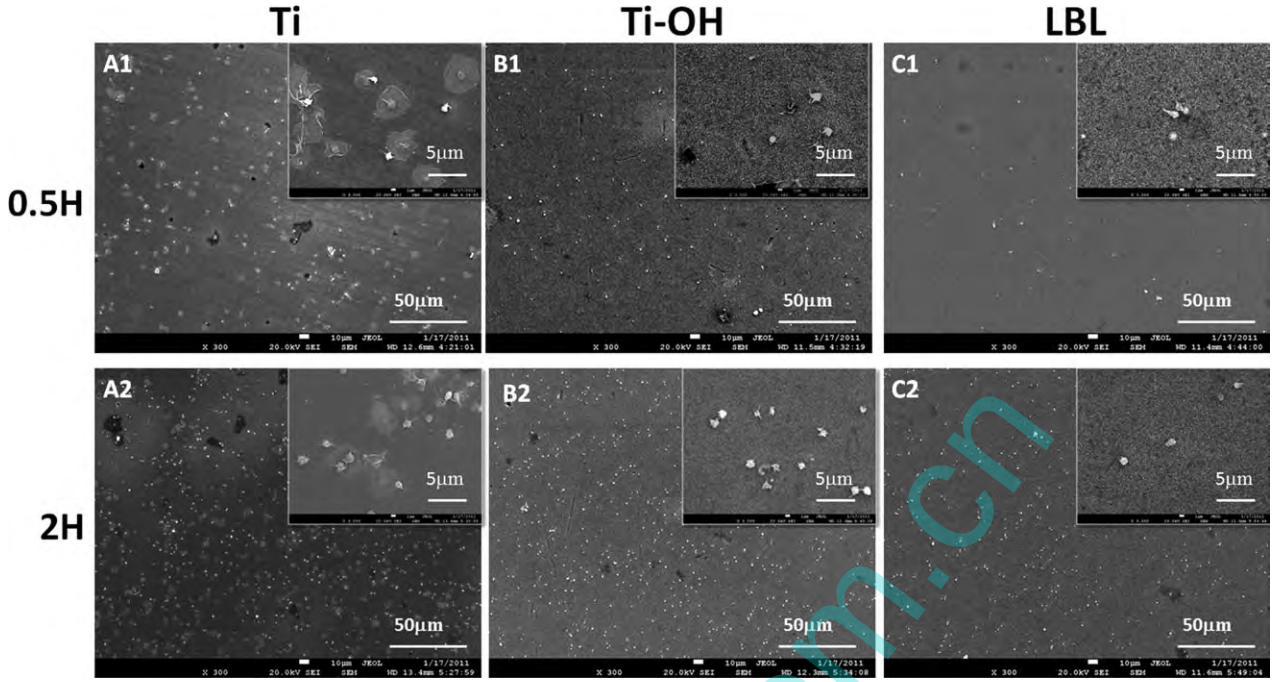

FIGURE 10. SEM images of platelets adhesion on different samples with (A1 and A2) Ti, (B1 and B2) Ti–OH, and (C1 and C2) LBL [incubation time: (A1, B1, and C1) 0.5 h and (A2, B2, and C2) 2 h].

with the LBL-assembled layer, the lowest ratio (19%) of activated platelets is presented.

Activated partial thromboplastin time

The APTT measurement is often used for judging the presence and effect of antithrombotic medicine, such as heparin and heparin-like drugs, according to the prolongation of APTT. Figure 14 shows the measured APTT values of the different samples. The APTT of the PPP was also measured for comparison. APTT was significantly prolonged on the LBL-assembled samples compared with that of Ti and Ti–OH samples. The APTT of LBL-assembled samples extend approximately 20 s compared with that of PPP, whereas on the reference Ti and Ti–OH samples it was only slightly prolonged.

DISCUSSION

Thrombosis and restenosis are the main limitations of coronary artery stents.[34] Re-endothelialization is essential for restoration of normal vascular homeostasis and prevention of thrombosis.[34] Recently, the EPC, which emerged as an important component of the response to vascular injury, has the potential to accelerate vascular repair through rapid re-endothelialization.[34] *In situ* rapid re-endothelialization, endothelium repaving, or relining at denudated regions after stent implantation has been proposed and attempted by surface modification in recent years.[35,36]

Surface chemical composition, morphology, roughness, and hydrophilicity strongly affect cellular responses in contact with the implants. Many studies have disclosed the important influence of physicochemical properties especially surface roughness on implant success.[37] It has been well known that the natural vascular tissue possesses a large degree of nanometer roughness due to the presence of nanostructured extracellular matrix proteins such as collagen and elastin. Therefore, many researchers try to create unique nanometer topography by mimicking the structure of natural vascular tissue. In this work, the biofunctional layers were assembled on alkaline etching titanium surface which shows nanometer roughness about 40–60 nm using AFM detection (Table I). It is reported that changes in surface chemistry or roughness of the same dimension as a protein would affect its adsorption characteristics. Instead,

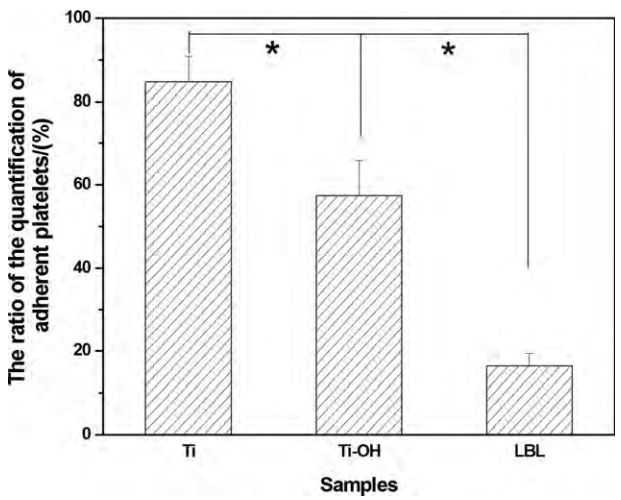

FIGURE 11. The ratio of the quantification of adherent platelets on different samples (the total lysed platelet suspensions that used to make calibration curve is taken as 100%) ($N = 4$, mean ± std, and $*p < 0.05$).

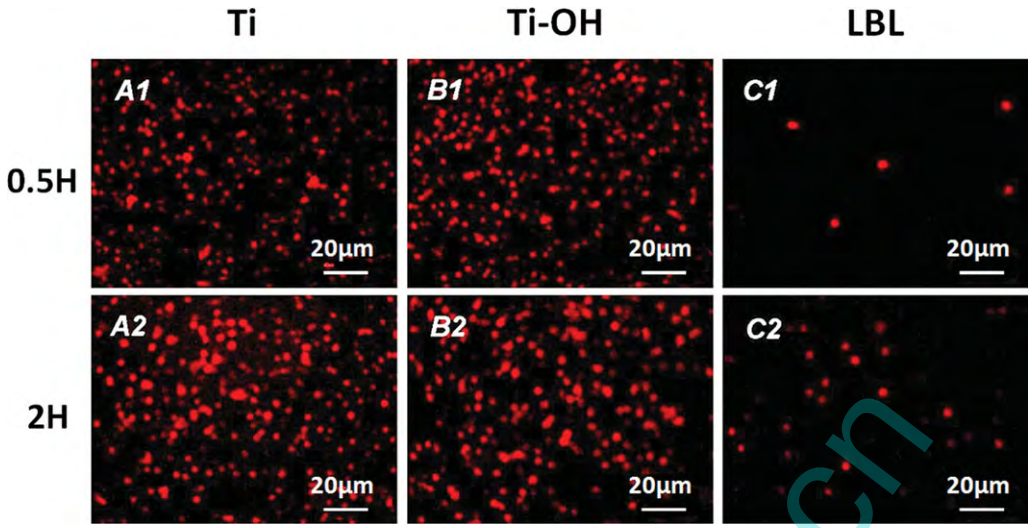

FIGURE 12. GMP-140 immunofluorescence images of platelets activation on different samples with (A1 and A2) Ti, (B1 and B2) Ti–OH, (C1 and C2) LBL [incubation time: (A1, B1, and C1) 0.5 h and (A2, B2, and C2) 2 h]. [Color figure can be viewed in the online issue, which is available at wileyonlinelibrary.com.]

if the rough surface is chemically homogeneous and the size of asperities was larger than that of the protein dimension, then roughness would simply add available surface area for adsorbing protein and subsequently enhance cell adhesion.[30] Comparing to conventional Ti, however, the nanostructured Ti–OH shows a bit limitation of EPCs adhesion and proliferation (Figs. 9 and 10). The factual result is different from other researcher's conclusion that nanostructured surface could improve EC growth.[37,38] It may partly due to the Ti–OH surface represent superhydrophilic characteristic, which may facilitate the formation of a compact water film on material surface after immersed into cell suspension and thereby inhibit adhesive proteins adsorption and subsequently reduce cell adhesion. Some researchers also demonstrated that the adsorption behavior onto hydrophilic surfaces is reversible and proteins can be displaced.[39] In contrast, alkali treated Ti surface exposes negatively charged hydroxyl, which may also inhibit the adhesion of negative charged protein and EPCs, as well as platelets. These explanations had been partly proved by platelets adhesion and activation experiments results (Figs. 11–14).

Surface antithrombosis modification by physical or chemical methods could improve the hemocompatibility of stents, while these methods may also lead to delayed endothelialization. More and more strategies aim to coat stent surface with a ECs-compatible bioactive protein layer, which can stimulate the attachment and proliferation of the surrounding mature ECs and the circulating EPCs to stents' surface, and thus accelerate the formation of an active ECs layer after prostheses implantation. In this work, we assembled anti-CD34 antibody–VEGF–heparin on NaOH

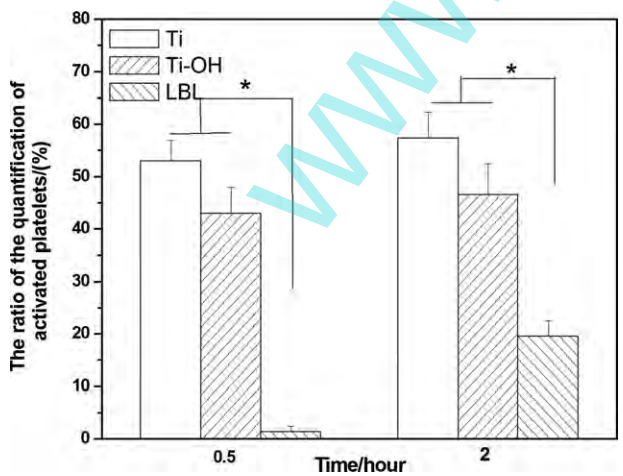

FIGURE 13. The ratio of the quantification of activated platelets on different samples (the initial concentration of HRP labeled antibody that used to make standard curve is taken as 100%) ($N = 4$, mean ± std, and $^*p < 0.05$).

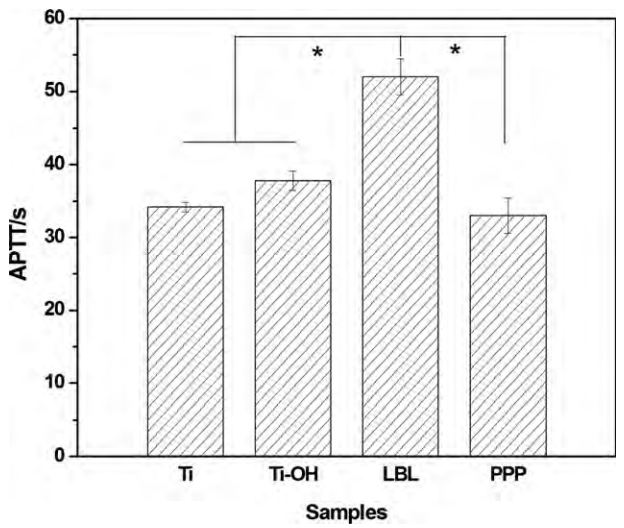

FIGURE 14. The measured results of activated partial thromboplastin time (APTT) on different samples surface ($N = 4$, mean ± std, and $^*p < 0.05$).

treated titanium surface to obtain the optimal EPCs adhesion and proliferation. The CD34 molecule is one sort of cell surface antigen, which is specifically presented on the vascular ECs, EPCs, and hematopoietic progenitor cells. Numerous studies have demonstrated that the immobilization of anti-CD34 antibody on stent surfaces contribute to EPCs adhesion and endothelium formation. According to Min Yin's research,[40] cells attachment increases with the increasing of anti-CD34 antibody concentrations, the cells attached on the samples-coated antibody increase approximately 25% when the concentration of antibody is 2 μg/mL. Moreover, it is reported that the antibody at the density of 1 $\mu g/cm^2$ can combine with 10^6 cells.[41] Herein assembled the anti-CD34 antibody at the concentration of 2 μg/mL and the mass of successfully assembled anti-CD34 antibody and VEGF achieve the requirement for cells attachment. Relating to CD34 antibody immobilization, however, some studies show that if taken random immobilization, the antibodies may be lost activities for binding sites shielding due to space resistance, 90% of monoclonal antibodies and 75% of polyclonal antibody would be deactivated.[42] So, finding an effective antibodies immobilization method to achieve maximum bioactivities is the most important. In our previous article,[25] biotinylated protein A was found to bind Fc (constant region) fragments of antibodies specially. Herein, we use biotinylated protein A and the biotinylated heparin to immobilize the anti-CD34 antibody and VEGF, respectively, which is based on the specific binding of protein A and Fc segments of CD34 antibody and the specific affinity of heparin and VEGF. The results in Figure 9 show the anti-CD34 antibody–VEGF–heparin multilayer improve the EPCs attachment and proliferation. After 5 days culture, a cell monolayer formed on the LBL sample surface, which shows rapid endothelialization.

In addition, VEGF also plays an important role in EPCs great behavior on LBL surface. Surface immobilized VEGF can mediate cell adhesion and migration via interaction with its corresponding transmembrane receptors, such as integrins αvβ3, α3β1, and α9β1.[43] More importantly, immobilized VEGF retained activity to induce the dimerization and phosphorylation of its specific tyrosine kinase receptor VEGFR-2, and then trigger a series of downstream signaling pathways such as PI3K/Akt and MAPK/ERK signaling pathway to promote the proliferation, migration, differentiation, and survival of cells. Therefore, assembling anti-CD34 antibody and VEGF can enrich and accelerate the attachment and proliferation of the EPCs, and promote the differentiation of cells, also induce the surface endothelialization onto Titanium surface.

Moreover, the *in vitro* platelet experiment result show the LBL-assembled layer have better antiadherent and antiactivation for platelet. That is because heparin has significant effect on platelet behavior. Heparin is a kind of glycosaminoglycan rich in carboxyl, sulfanilamide, and sulfonic group and has been the most widely used anticoagulant in clinical. The negative charge of heparin cause an electrostatic repulsion to inhibit the adhesion of negatively charged platelets, and heparin may also block the active site of glycoproteins which mediate platelet adhesion. Adachi et al.[44] discussed the mechanism of heparin block platelets adhesion at the molecular level, they suggested that heparin can rapidly bind the active site of vWF, a glycoprotein that mediate platelet adhesion by interaction with platelet glycoprotein Ib (GPIb), thereby inhibit the formation of complex vWF–GPIb and reduce platelets adhesion ultimately.

In addition, the anticoagulation function of heparin was achieved by several routes and the exact physiological role in the body remains unclear, while it was generally accepted that the potency of heparin was mainly depend on its binding activity to antithrombin III (AT III). AT III is an important plasma cofactor that inactivates thrombin and can strongly bind to the specific pentasaccharide structure of heparin via its lysine residues.[45] The conformation changes of AT III occur in response to the binding of heparin, which may enhance the combination of AT III to the serine active site of thrombin, and thereby facilitate the ternary complex thrombin–AT III–heparin formation. It has been well demonstrated that the rate of AT III–thrombin inactivation is increased 2000–4000-fold in the presence of heparin.[46,47] According to APTT result (Fig. 14), it can be concluded that Ti and Ti–OH samples have no significant effect on the activity of AT III, whereas the assembled heparin retained its activity and the thrombin–AT III–heparin complex was formed induced by LBL. In this way, plasma thrombin lost its activity to catalyze the conversion of the soluble plasma protein fibrinogen to the insoluble protein fibrin. The assembled layer shows great hemocompatibility.

CONCLUSIONS

In this article, for improving the compatibility of Titanium surface, a biofunctional layer with anti-CD34 antibody, VEGF and heparin are successfully fabricated on the negative charge titanium surface treated with NaOH solution by a LBL self-assembly technique. The assembled layer shows nanometer morphology and hydrophilicity. The *in vitro* EPCs culture results prove that, comparing to the controlling Ti and Ti–OH surface, the LBL greatly promote the adhesion, proliferation and supersession of EPCs. The *vitro* platelet experiment and APTT measurement results clearly demonstrate that, the LBL multilayer inhibits the adhesion, aggregation and activation of platelet and extends the APTT. It can be concluded that, a biofunctional LBL on Titanium surface, constructed by assembling the anti-CD34 antibody, VEGF, and heparin, could significantly improve the endothelialization and anticoagulation of titanium surface.

REFERENCES

1. Hong J, Andersson J, Ekdahl KN, Elgue G, Axen N, Larsson R, Nilsson B. Titanium is a highly thrombogenic biomaterial: Possible implications for osteogenesis. Thromb Haemost 1999;82:58–64.
2. Asahara T, Murohara T, Sullivan A, Silver M, van der Zee R, Li T, Witzenbichler B, Schatteman G, Isner JM. Isolation of putative progenitor endothelial cells for angiogenesis. Science 1997;275:964–967.
3. Calzi SL, Neu MB, Shaw LC, Kielczewski JL, Moldovan NI, Grant MB. EPCs and pathological angiogenesis: When good cells go bad. Microvasc Res 2010;79:207–216.
4. Avci-Adali M, Paul A, Ziemer G, Wendel HP. New strategies for in vivo tissue engineering by mimicry of homing factors for self-

endothelialization of blood contacting materials, Biomaterials 2008;29:3936–3945.
5. Kutryk MJ, Kuliszewski MA. In vivo endothelial progenitor cell seeding for the accelerated endothelialization of endovascular devices. Am J Cardiol 2003;92(6A):94L–95L.
6. Aoki J, Serruys PW, van Beusekom H, Ong AT, McFadden EP, Sianos G, van der Giessen WJ, Regar E, de Feyter PJ, Davis HR, Rowland S, Kutryk MJ. Endothelial progenitor cell capture by stents coated with antibody against anti-CD34: the HEALING-FIM (healthy endothelial accelerated lining inhibits neointimal growth-first in man) registry. J Am Coll Cardiol 2005;45:1574–1579.
7. Rotmans JI, Heyligers JM, Verhagen HJ, Velema E, Nagtegaal MM, de Kleijn DP, de Groot FG, Stroes ES, Pasterkamp G. In vivo cell seeding with anti-CD34 antibodies successfully accelerates endothelialization but stimulates intimal hyperplasia in porcine arteriovenous expanded polytetrafluoroethylene grafts. Circulation 2005;112:12–18.
8. Pitchford SC, Furze RC, Jones CP, Wengner AM, Rankin SM. Differential mobilization of subsets of progenitor cells from the bone marrow. Cell Stem Cell 2009;4:62–72.
9. Krenning G, van Luyn MJ, Harmsen MC. Endothelial progenitor cell-based neovascularization: implications for therapy. Trends Mol Med 2009;15:180–189.
10. Asahara T, Takahashi T, Masuda H, Kalka C, Chen D, Iwaguro H, Inai Y, Silver M, Isner JM. VEGF contributes to postnatal neovascularization by mobilizing bone marrow-derived endothelial progenitor cells. EMBO J 1999;18:3964–3972.
11. Crombez M, Chevallier P, Gaudreault RC, Petitclerc E, Mantovani D, Laroche G. Improving arterial prosthesis neo-endothelialization: Application of a proactive VEGF construct onto PTFE surfaces. Biomaterials 2005;26:7402–7409.
12. Pike DB, Cai SS, Pomraning KR, Firpo MA, Fisher RJ, Shu XZ, Prestwich GD, Peattie RA. Heparin-regulated release of growth factors in vitro and angiogenic response in vivo to implanted hyaluronan hydrogels containing VEGF and bFGF. Biomaterials 2006;27:5242–5251.
13. Christensen K, Larsson R, Emanuelsson H, Elgue G, Larsson A. Heparin coating of the stent graft—Effects on platelets, coagulation and complement activation. Biomaterials 2001;22:349–355.
14. Gong F, Cheng X, Wang S, Zhao Y, Gao Y, Cai H. Heparin-immobilized polymers as non-inflammatory and non-thrombogenic coating materials for arsenic trioxide eluting stents. Acta Biomater 2010;6:534–546.
15. Lin PH, Bush RL, Yao Q, Lumsden AB, Chen C. Evaluation of platelet deposition and neointimal hyperplasia of heparin-coated small-caliber ePTFE grafts in a canine femoral artery bypass model. J Surg Res 2004;118:45–52.
16. Li QL, Huang N. Endothelial cell and platelet behavior on titanium modified with a mutilayer of polyelectrolytes. J Bioact Compat Polym 2009;24:129–150.
17. Meng S, Liu ZJ, Shen L, The effect of a layer-by-layer chitosan–heparin coating on the endothelialization and coagulation properties of a coronary stent system. Biomaterials 2009;30: 2276–2283.
18. Lu DL, Meng S, Zhong W, Du QG, Li G, Liu JF, Dusan B. Immobilization of biomacromolecules on poly-L-lactide surface via a layer-by-layer method for the improving of its cytocompatibility to bone marrow stromal cells. Chin Sci Bull 2005;50: 2809–2816.
19. Weng YJ. Surface Modification of Ti–O film by antithrombotic biomolecule immobilization and evaluation of its antithrombotic properties. Southwest Jiaotong University Doctor Degree Dissertation; 2004.
20. Chen C, Chen JY, Li QL, Chen JL, Tu QF, Chen SM, Liu SH, Huang N. The biological behavior of endothelial progenitor cells on titanium surface immobilized by anti-CD34 antibody. Adv Mater Res 2009;9–82:707–710.
21. Tokunaga Y, Yamazaki Y, Morita T. Localization of heparin-and neuropilin-1-recognition sites of viral VEGFs. Biochem Biophys Res Commun 2006;348:957–962.
22. Kujawa P, Schmauch G, Viitala T, Badia A, Winnik FM. Construction of viscoelastic biocompatible films via the layer-by-layer assembly of hyaluronan and phosphorylcholine-modified chitosan. Biomacromolecules 2007;8:3169–3176.
23. Lin Q, Ding X, Qiu F, Song X, Fu G, Ji J. In situ endothelialization of intravascular stents coated with an anti-CD34 antibody functionalized heparin–collagen multilayer. Biomaterials 2010;31: 4017–4025.
24. Cui X, Pei R, Wang Z, Yang F, Ma Y, Dong S, Yang X. Layer-by-layer assembly of multilayer films composed of avidin and biotin-labeled antibody for immunosensing. Biosen Bioelectron 2003;18: 59–67.
25. Li QL, Huang N, Chen C, Chen JL, Xiong KQ, Chen JY, You TX, Jin J, Liang X. Oriented immobilization of anti-CD34 antibody on titanium surface for self-endothelialization induction. J Biomed Mater Res A 2010;94:1283–1293.
26. Hou RX, Wu LG, Wang J, Huang N. Investigation on biological properties of tacrolimus-loaded poly(1,3-trimethylene carbonate) in vitro. Appl Surf Sci 2010;256:5000–5005.
27. Yang ZL, Wang J, Luo RF, Maitz MF, Jing F, Sun H, Huang N. The covalent immobilization of heparin to pulsed-plasma polymeric allylamine films on 316L stainless steel and the resulting effects on hemocompatibility. Biomaterials 2010;31:2072–2083.
28. Chen JL, Li QL, Chen JY, Chen C, Huang N. Improving blood-compatibility of titanium by coating collagen–heparin multilayers. Appl Surf Sci 2009;255:6894–6900.
29. Pradier CM, Salmain M, Zheng L, Jaouen G. Specific binding of avidin to biotin immobilised on modified gold surfaces Fourier transform infrared reflection absorption spectroscopy analysis. Surf Sci 2002;502–503:193–202.
30. Chung TW, Liu DZ, Wang SY, Wang SS. Enhancement of the growth of human endothelial cell by surface roughness at nanometer scale. Biomaterials 2003;24:4655–4661.
31. Oikawa Y, Minami T, Mayama H, Tsujii K, Fushimi K, Aoki Y, Skeldon P, Thompson GE, Habazaki H. Preparation of self-organized porous anodic niobium oxide microcones and their surface wettability. Acta Mater 2009;57:3941–3946.
32. Feng B, Weng J, Yang BC, Chen JY, Zhao JZ, He L, Qi SK, Zhang XD. Surface characterization of titanium and adsorption of bovine serum albumin. Mater Charact 2003;49:129–137.
33. Li GC, Zhang FM, Liao YZ, Yang P, Huang N. Coimmobilization of heparin/fibronectin mixture on titanium surfaces and their blood compatibility. Colloid Surf B Biointerfaces 2010;81:255–262.
34. Padfield GJ, Newby DE, Mills NL. Understanding the role of endothelial progenitor cells in percutaneous coronary intervention. J Am Coll Cardiol 2010;55:1553–1562.
35. Parikh SA, Edelman ER. Endothelial cell delivery for cardiovascular therapy. Adv Drug Deliver Rev 2000;42:139–161.
36. Shirota T, Yasui H, Shimokawa H, Matsuda T. Fabrication of endothelial progenitor cell (EPC)-seeded intravascular stent devices and in vitro endothelialization on hybrid vascular tissue. Biomaterials 2003;24:2295–302.
37. Choudhary S, Haberstroh KM, Webster TJ. Enhanced functions of vascular cells on nanostructured Ti for improved stent applications. Tissue Eng 2007:1421–1430.
38. Ponsonnet L, Reybier K, Jaffrezic N, Comte V, Lagneau C, Lissac M, Martelet C. Relationship between surface properties (roughness, wettability) of titanium and titanium alloys and cell behaviour. Mater Sci Eng C 2003;23:551–560.
39. van Wachem PB, Vreriks CM, Beugeling T, Feijen J, Bantjes A, Detmers JP, van Aken WG. The influence of protein adsorption on interactions of cultured human endothelial cells with polymers. J Biomed Mater Res A 1987;21:701–718.
40. Yin M, Yuan Y, Liu CS, Wang J. Combinatorial coating of adhesive polypeptide and anti-CD34 antibody for improved endothelial cell adhesion and proliferation. J Mater Sci Mater Med 2009;20: 1513–1523.
41. McSweeney PA, Rouleau KA, Wallace PM, Bruno B, Andrews RG, Krizanac-Bengez L, Sandmaier BM, Storb R, Wayner E, Nash RA. Characterization of monoclonal antibodies that recognize canine CD34. Blood 1998;91:1977–1986.
42. Butler JE, Ni L, Brown WR, Joshi KS, Chang J, Rosenberg B, Voss EW. The immunochemistry of sandwich ELISAs—VI. Greater than 90% of monoclonal and 75% of polyclonal anti-fluorescyl capture antibodies (CAbs) are denatured by passive adsorption. Mol Immunol 1993;30:1165–1175.
43. Ferrara N. Vascular endothelial growth factor: basic science and clinical progress. Endocr Rev 2004;25:581–611.

44. Adachi T, Matsushita T, Dong ZY, Katsumia A, Nakayamaa T, Kojimac T, Saitod H, Sadlerb JE, Naoea T. Identification of amino acid residues essential for heparin binding by the A1 domain of human von Willebrand factor. Biochem Biophys Res Commun 2006;339:1178–1183.
45. Blackburn MN, Smith RL, Carson J, Sibley CC. The heparin-binding site of antithrombin III. Identification of a critical tryptophan in the amino acid sequence. J Biol Chem 1984;259: 939–941.
46. Olson ST, Bjork I. Predominant contribution of surface approximation to the mechanism of heparin acceleration of the antithrombin–thrombin reaction. Elucidation from salt concentration effects. J Biol Chem 1991;26:6353–6364.
47. Olson ST, Bjork I, Sheffer R, Craig PA, Shore JD, Choay J. Role of the antithrombin-binding pentasaccharide in heparin acceleration of antithrombin–proteinase reactions. Resolution of the antithrombin conformational change contribution to heparin rate enhancement. J Biol Chem 1992;267:12528–12538.